

Side Group Rotational Mobility in Hairy-Rod Polymers: A Dielectric Spectroscopy Study

M. Bockstaller,[†] G. Fytas,^{*,†,‡} and G. Wegner[†]

Max-Planck-Institute for Polymer Research, P.O. Box 3148, 55128 Mainz, Germany, and FORTH–Institute of Electronic Structure and Laser, P.O. Box 1527, 71110, Heraklion, Crete, Greece

Received October 30, 2000

Synthetic shape persistent polymers bear side chains to enhance solubility in common solvents necessary for processing from solutions.¹ A pertinent property of this class of materials is the anisotropic translational diffusion and the translational–rotational coupling in nondilute solutions.² In the theoretical descriptions, the presence of side groups implicitly enters into an effective chain diameter. The side group mobility and its relation to the chain backbone dynamics, in view of the complexity of the latter, are rarely addressed.

Substituted poly(*p*-phenylene) (PPPS) hairy-rod polymers with persistence length $l \approx 20$ nm have shown over a broad concentration range (up to 65 wt %) complex orientation dynamics,³ which relates to collective rotational motion of the Kuhn segments as measured by depolarized light scattering. Here the orientation motion of the aromatic sulfonated side groups (two per monomer unit, see the structure in the inset of Figure 1) of PPPS with different lengths is probed by dielectric spectroscopy (DS) in the megahertz–gigahertz frequency range to complement a recent dynamic depolarized light scattering study emphasizing backbone motions.³

Figure 1 shows the dielectric loss $\epsilon''(\omega)$ spectra of three PPPS samples with different molecular weight corresponding to contour length $L_n = 11$ (S10), 30 (S7), and 134 nm (S1) in toluene at similar concentrations (~ 22 wt %) at 20 °C. The complex dielectric permittivity $\epsilon^* = \epsilon' - i\epsilon''$ was measured with the Solartron-Schlumberger FRAU 1260 frequency response analyzer and a condenser cell over the frequency range 10^{-2} – 10^6 Hz. For measurements in the high-frequency range (10^6 – 10^9 Hz) a network analyzer HP 4191A has been employed. At first glance, a few observations emerge from Figure 1. (i) The peak position of $\epsilon''(\omega)$ yielding the characteristic relaxation frequency f_r does not decrease with polymer length. Instead, it is lower in the rodlike S10. (ii) The peak amplitude increases from the semiflexible S1 toward rigid S10. (iii) The experimental $\epsilon''(\omega)$ are broader than a single Debye (solid line) function for all three chain lengths. The representation of $\epsilon''(\omega)$ by the empirical Havriliak–Negami⁴

$$(\epsilon^*(\omega) - \epsilon_\infty)/\Delta\epsilon = [1 + (i\omega\tau)^\alpha]^{-\gamma} \quad (1)$$

yields the relaxation strength $\Delta\epsilon$, the characteristic time τ , and the exponents α and γ which describe the broadening of the distribution of relaxation times. Using a fixed $\gamma = 1$, the distribution can be described by $\alpha = 0.6 \pm 0.1$ and the relaxation time τ assumes 13, 9, and 6 ± 1 ns for S10, S7, and S1 whereas in the same order

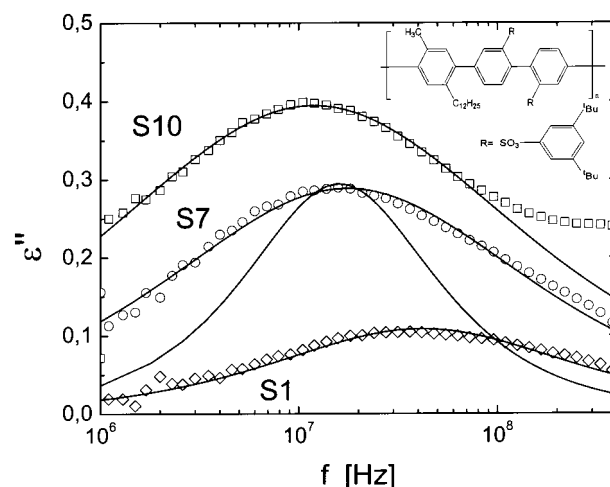


Figure 1. Dielectric loss spectra of three PPPS with number-average molecular weight $M_n = 8150$ (S10), 22 000 (S7), and 99 900 g/mol (S1) in toluene with similar concentration (~ 22 wt %) at 293 K. The solid lines represent Havriliak–Negami fits, and the spectra are broader than a single Debye function (solid line). Inset: the chemical structure of the repeated unit.

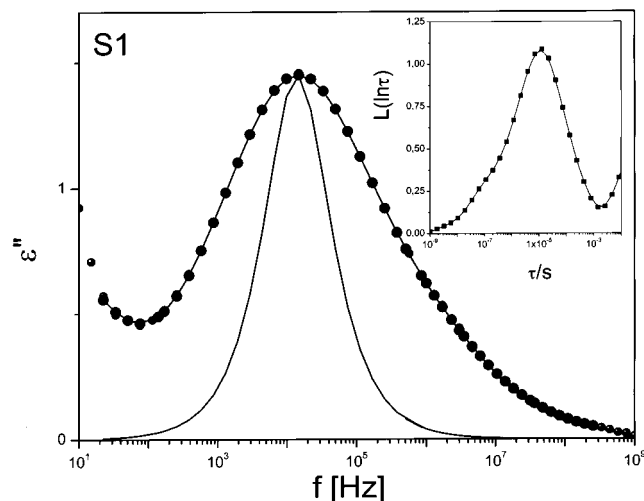


Figure 2. Dielectric loss spectrum of S1 at 55 wt % in toluene at 20 °C. The distribution of relaxation times $L(\ln \tau)$ (eq 2) is shown in the inset. The spectrum is clearly broader than a single Debye function (solid line).

the strength $\Delta\epsilon$ decreases from 1.6, to 1.1, to 0.4 ± 0.1 at 293 K. Since the dipole moment is directed along the side groups R (inset of Figure 1), the observed dielectric relaxation reflects their local rotational dynamics, which is insensitive to the variation of the macromolecular size. The PPPS solutions of Figure 1 are in the semidilute regime but not equidistant from the overlap concentration c^* (Table 1, ref 3); $c/c^* = 2, 5.5$, and 11 for S10, S7, and S1 solutions. Hence, the nonexponential shape and the different $\Delta\epsilon$ might arise from interchain interactions in addition to intrachain correlations. To address this possibility, the effect of concentration on the experimental $\epsilon''(\omega)$ should be examined (see Figure 3).

The spectrum for the highest concentration (55 wt %) of S1 recorded by comprising two frequency ranges shows that a single broad rather than a bimodal distribution relaxation function is more appropriate for

[†] Max-Planck-Institute for Polymer Research.

[‡] FORTH–Institute of Electronic Structure and Laser.

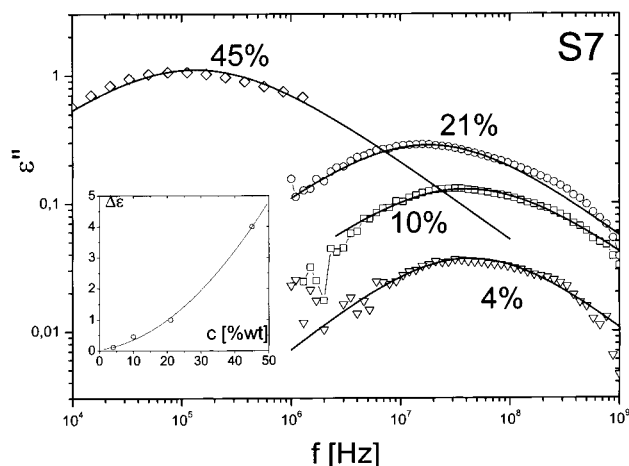


Figure 3. Dielectric loss spectra of S7 for four concentrations in toluene at 20 °C. The dispersion $\epsilon''(\omega)$ for the highest concentrations has been measured over a broad frequency range. The variation of the dielectric strength as obtained from the HN fit (solid lines) with concentration is shown in the inset.

the non-Debye shape of $\epsilon''(\omega)$ in Figure 2. This is illustrated in the inset of Figure 2, which shows the unimodal distribution of relaxation times $L(\ln \tau)$ extracted from the inversion of

$$\epsilon''(\omega) = \int_{-\infty}^{\infty} L(\ln \tau) [\omega \tau / (1 + \omega^2 \tau^2)] d(\ln \tau) \quad (2)$$

assuming a superposition of Debye functions;⁵ below about 10^{-3} s the rise is due to the electrical conductivity in $\epsilon''(\omega)$.

The concentration dependence of $\epsilon''(\omega)$ for S7/toluene solutions in the range 4–45 wt % is shown in Figure 3. The distribution relaxation function experiences a weak broadening with concentration at constant temperature since the value of the width of the distribution of relaxation times α (eq 1) decreases slightly from 0.70 to 0.63 ± 0.1 for 4% and 45 wt % S7/toluene solutions; for comparison, the decrease of temperature has a more pronounced broadening effect. The deviation from the single-exponential ($\alpha = \gamma = 1$) orientation relaxation, already present at 4%, along with the weak variation of f_r with S7 concentration up to 21 wt % (in contrast to the change of the solution viscosity), favors the importance of intrachain conformational correlations on the heterogeneity⁶ of the local side group rotational motion; intermolecular effects would, on the contrary, impede the motion with solute concentration. The abrupt slowing down of f_r above 21 wt % and the concurrent increase of $\Delta\epsilon/c$ (inset of Figure 3) can therefore be ascribed to interchain collective effects. The cooperativity of the side group orientation dynamics at high concentrations is further supported by the increase of the Arrhenius activation energy E_a of τ ; E_a increases from 35 to 48 ± 4 kJ/mol for 21 and 33 wt % S1 in toluene.

The concentration dependence of the side group orientation time is depicted in Figure 4 along with the characteristic rotational times obtained from the dynamic depolarized light scattering.³ The latter has revealed two distinct nonexponential processes associated with the collective backbone rotational motion on the length scale of Kuhn segments. The overall rotation time measured by dynamic rheometry (shown for S1/toluene solution in Figure 4) is even slower. This relaxation map is a manifestation of the widely spread

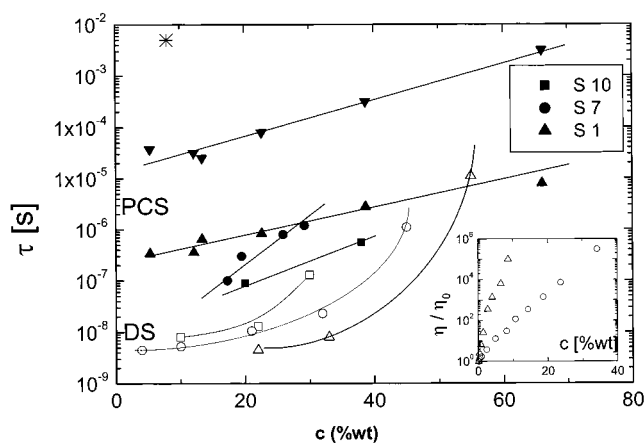


Figure 4. Orientation relaxation times in three PPPS hairy rods as a function of polymer concentration in toluene. Dielectric spectroscopy (DS): open symbols. Depolarized light scattering (PCS):³ solid symbols for the fast and inverse triangle for the slow process (only for S1). The longest relaxation time (overall chain rotation) from dynamic rheometry is also shown for S1 (*). Inset: normalized shear viscosity³ for S1 and S7 vs concentration. Lines are drawn to guide the eye.

time scales of the orientation dynamics in these persistent polymers as probed by three experimental techniques.

The pertinent finding of Figure 4 is the closeness of the backbone and side group orientation dynamics at concentrations higher than about 40 wt %, suggesting that the rate-determining step for the latter is the segmental mobility. The crossover concentrations for this local backbone–side group dynamic coupling appear to relate to chain rigidity since it increases from S10 to S1. At lower concentrations short molecular displacements not sufficient to relax segmental orientation fluctuations can allow side group rotation, and hence these motions occur at distinctly different times for all samples. Further they display a weaker concentration dependence than that of the solution shear viscosity. The latter relates to the slow overall chain motion (shown for S1 in Figure 4). The origin of the slow process in the depolarized light scattering³ (shown only for S1) that exhibits a peculiar wave vector dependence is not known. In view of the data of Figure 4, this slow mode might reflect motions of orientationally correlated Kuhn segments.

Finally, anisotropic side chain dynamics were observed in liquid crystalline polymers.⁷ Recently, the broad dielectric loss spectra of fluorocarbon groups in ordered diblock copolymers⁸ and undiluted carbosilane dendrimers⁹ have shown evidence of the presence of a bimodal orientation relaxation function. Microscopically, these are probably related to the dipolar components parallel and perpendicular to the long axis of the fluorocarbon group. The present PPPS solutions are in the isotropic state over the examined concentration range, the nonexponential decay of the side group orientation relaxation function is unimodal, and the single but non-Debye $\epsilon''(\omega)$ (eq 2) can be used as a heterogeneity index of the side group local environment. Interestingly enough, the motional rates for side group and segmental orientation become very similar above about 40 wt %.

Acknowledgment. We acknowledge the financial support of the European Union (Grant HPRN-CT2000-00003).

References and Notes

- (1) Vanhee, S.; Rülkens, R.; Lehmann, U.; Rosenauer, C.; Schulze, M.; Köhler, W.; Wegner, G. *Macromolecules* **1996**, *29*, 5136.
- (2) Doi, M.; Edwards, S. F. *The Theory of Polymer Dynamics*; Oxford University Press: New York, 1986. Sato, T.; Teramoto, A. *Adv. Polym. Sci.* **1996**, *126*, 85.
- (3) Petekidis, G.; Vlassopoulos, D.; Fytas, G.; Rülkens, R.; Wegner, G. *Macromolecules* **1998**, *31*, 6129; **2000**, in press.
- (4) Havriliak, S.; Negami, S. *Polymer* **1967**, *8*, 161.
- (5) Karatasos, K.; Anastasiadis, S. H.; Semenov, A. N.; Fytas, G.; Pitsikalis, M.; Hadjichristidis, N. *Macromolecules* **1994**, *27*, 3543.
- (6) This dynamic heterogeneity bears some analogy to the distinct component mobilities in polymer mixtures. Doxastakis, M.; et al. *J. Chem. Phys.* **2000**, *112*, 8687.
- (7) Cremer, Ch.; Cremer, Th.; Kremer, F.; Stannarius, R. *J. Chem. Phys.* **1997**, *106*, 3730.
- (8) Floudas, G.; Antonietti, M.; Förster, S. *J. Chem. Phys.* **2000**, *113*, 3447.
- (9) Trabasch, B.; Stühn, B.; Frey, H.; Lorenz, K. *Macromolecules* **1999**, *32*, 1962.

MA001863F